Coastal Engineering 117 (2016) 166–175

Contents lists available at ScienceDirect

Coastal Engineering

journal homepage: www.elsevier.com/locate/coastaleng

A parametric model for barred equilibrium beach profiles: Two-dimensional implementation

Robert A. Holman *, David M. Lalejini, Todd Holland

Marine Geosciences Division, Naval Research Laboratory, Code 7434, Bldg 1005, Stennis Space Center, MS 39529-5004, USA

ARTICLE INFO

Article history:
Received 14 January 2016
Received in revised form 9 May 2016
Accepted 28 July 2016
Available online 1 September 2016

Keywords:
Bathymetry estimation
Remote sensing
Nearshore
Equilibrium beach
Parametric profiles

ABSTRACT

A method is proposed for estimating approximate 2DH bathymetry including longshore variable shoreline and sand bar systems. The method is based on, but extends, a previous 1DH model of Holman et al. (2014) by assuming that this 1DH equilibrium barred bathymetry can be applied for any offshore location if the corresponding mean shoreline orientation is taken to be the local average over a longshore span that is K times the offshore distance. Thus locations close to the beach are sensitive to shoreline and bar details while more seaward locations are steadily less sensitive.

The model was tested against 14 ground truth surveys, collected over two years and under widely ranging environmental condition, spanning a 500 by 1000 m region. Models inputs for the shoreline and sand bar positions were extracted from measured bathymetries for these tests (but would be derived from other sources in real applications) while deep-water inputs were found from a single deep-water survey. The model yielded complete 2DH bathymetry maps that were a very good approximation of ground truth. The mean bias and rms error over the full region and data set were 0.27 m and 0.49 m respectively and proxy bathymetries were visually very similar to ground truth. The largest source of error was occasional cross-shore misplacements of otherwise realistic looking sand bars. Results were only weakly dependent on the value of K when tested over a factor of four and the default value of 1.0 is recommended. Performance statistics using input locations for the shoreline and bar crest that were manually digitized from breaking patterns in rectified optical time exposure images were no worse than bathymetry-based inputs. Hydrodynamic predictions using these bathymetries would be a substantial improvement over those from monotonic or even barred 1DH equilibrium proxy bathymetries.

Published by Elsevier B.V.

1. Introduction

Parametric forms for equilibrium beaches have been studied and used for many years as plausible proxies for bathymetry for cases where the true bathymetry is unknown or is only poorly known, or for long-term applications such as beach response to sea level rise where it is assumed that only the gross characteristics of a beach such as increasing depth and upward concavity are important (see Ozkan-Haller and Brundidge, 2007 for a recent review). One of the most common models is the ubiquitous $h = Ax^{2/3}$ form, first introduced by Bruun (1954) then popularized by Dean (1991), where x and h are distance from shore and depth and A is a dimensional calibration constant. However, other forms soon followed. Inman et al. (1993) suggested a version that joined two Dean-like profiles at the breakpoint, Larson and Kraus (1989) suggested a form that superimposed a planar shallow water component with an offshore Dean form, Ozkan-Haller and Brundidge (2007) introduced a modification to further limit the influence of the planar component to shallow water, and Bodge (1992) and Komar and McDougal (1994) suggested exponential rather than power law forms as a preferred solution that exhibited finite slope at the shoreline and a desired concave up profile. All of these forms flattened to a horizontal surface offshore, hopefully well seaward of a zone in which they would be applied.

While all of these forms capture some characteristics of beaches, none can represent the near-ubiquitous presence of sand bars in the nearshore. Since wave dissipation is focused over bars, hydrodynamic predictions such as nearshore circulation or peak wave height made using beach profiles that omit these features will have limited value.

Ruessink et al. (2003; hereafter RWHKvE03) investigated the possibility of deriving a parametric form for sand bar perturbations to a simple background profile by analyzing extensive data sets from six beaches around the world and developing a general equation (described in the section below) that represented sand bars in terms of a sinusoidal function with spatially varying amplitude and wavelength. This bar function, h_{bar}, is superimposed on an underlying background bathymetry, h_0, that might be derived from long-term average

* Corresponding author.
E-mail addresses: holman@coas.oregonstate.edu (R.A. Holman), David.Lalejini@nrlssc.navy.mil (D.M. Lalejini), Todd.Holland@nrlssc.navy.mil (T. Holland).

http://dx.doi.org/10.1016/j.coastaleng.2016.07.010
0378-3839/Published by Elsevier B.V.

data or from one of the equilibrium equations noted above. Thus the total bathymetry would be

$$h(x,t) = h_0(x) + h_{bar}(h_0,t) \quad (1)$$

where they assumed no longshore variability.

In 2014, Holman et al. (2014; hereafter HLEV14) published a paper that merged the RWHKvE03 with a new background equilibrium form that combined an exponential, concave-up, nearshore form with a planar form offshore that better represents the steady deepening of the continental shelf seaward of the wave-influenced zone (method summarized in Section 2 of this paper). This equation improved the bathymetric representation for the many beach profiles tested from Duck, NC, beaches in the Pacific Northwest of the US, and from a Gulf of Mexico beach. Moreover, predictions of nearshore wave heights and longshore currents were considerably improved over predictions made on equilibrium profiles without sand bars.

The principal limitation of HLEV14 is the restriction to longshore uniform cases. While the paper suggests that "a 2DH morphology can reasonably be represented by an integrated set of adjacent 1DH slices", the details of this process turned out to not be trivial.

The purpose of this paper is to extend HLEV14 to allow for alongshore-variable bathymetry while maintaining simplicity of implementation and good fidelity with actual measured bathymetries. The next section will summarize the HLEV14 method for 1D barred beach representation. Section 3 will then introduce a method to extend the 1D case for 2D beaches based only on longshore estimates of the same simple parameters as were used in the 1D case. This is followed by a section testing the predictions against measurements for 14 example surveys from the Field Research Facility (FRF) at Duck, NC. Thereafter follow discussion and conclusions.

2. Model formulation

Since the 2D model is just an implementation of HLEV14, the next section will describe the 1D implementation from that paper while the following section will detail the new steps needed to expand to 2D. The reader is referred back to HLEV14 for greater detail on the 1D implementation.

2.1. The 1D HLEV14 profile model

The one-dimensional model requires specification of a background (unbarred) profile, h_0, and a barred perturbation function, h_{bar}, (Eq. (1)). For the background profile, HLEV14 proposed a mix of an exponential shoreward component to represent the concave up shapes of wave-formed profiles with a planar offshore region to represent geological shelf processes seaward of the wave-influenced zone,

$$h_0 = \alpha + \beta x + \gamma \exp(-kx). \quad (2)$$

where α, β, γ and k are empirical coefficients (β is dimensionless, α and γ have units m and k has units m^{-1}). They referred to this as a composite profile.

The four unknown coefficients were estimated using the following four pieces of information: 1, the shoreline position (essentially shifting to a shore-based coordinate system); 2, an equilibrium beach slope at the shoreline; 3, The depth at a specified position that is seaward of the active bar zone; and 4, the shelf slope at that location. The values of α and β are found directly while the values for γ and k must be found iteratively using Eqs. (5) and (7) from HLEV14.

The parametric form for the depth-dependent sand bar perturbation is taken from RWHKvE03

$$h_{bar}(h_0,t) = -S(h_0)R(t)\cos[\theta(h_0) - \psi(t)]. \quad (3)$$

The sand bar form is represented by the cosine and can be compared to the more familiar form of a progressive ocean wave, $\cos[kx - \sigma t]$, where k and σ represent the wavenumber and frequency of the wave. In this case, the spatial variability, kx, is replaced by a spatial phase function, $\theta(h_0)$ (solved in Eqs. (6) and (7) below), so is not a function of x directly but instead is a function of mean depth, h_0. The movement of the bar in time, represented by σt in a progressive wave, is represented by $\psi(t)$, a temporal phase function that is found by locating the bar crest at any time of interest (or any other feature – see HLEV14). $S(h_0)$ and $R(t)$ multiply the cosine so represent the amplitude of the cosine wave and how it varies in space (S) and in time (R).

From extensive survey data from six beaches in three countries, RWHKvE03 developed analytical forms for S, R and θ. They found that bar amplitude changes over time were small (i.e. bars change position much more than they grow or decay), so R(t) was set to 1.0. The spatial envelope of bar amplitude, $S(h_0)$ was well modeled by a skewed Gaussian of the form

$$S = \delta\frac{x}{x_{off}} + \left(S_{max} - \delta\frac{x_{max}}{x_{off}}\right)\exp\left[\frac{-\left\{\left(1-\frac{h_0-h_{shore}}{h_{sea}-h_{shore}}\right)^a - b\right\}^2}{c}\right] \quad (4)$$

where their original equations have been modified to remove the need to compensate for survey error in modeling parametric bathymetries (see HLEV14).

Bar amplitude depends on depth, h_0, everywhere in the transect rather than on x directly. The maximum amplitude of the Gaussian envelope is determined by S_{max} (RWHKvE03 adjusted Smax by a noise floor threshold, δ, taken empirically as 0.3 for survey data. Since there is no noise in parametric predictions, this is compensated for by the first term in Eq. (4)). h_{shore} and h_{sea} are the landward and seaward limits of significant bar activity (amplitude > δ) and h_{shore} can safely be set to zero for parametric applications. a, b and c are found empirically to be 0.53, 0.57 and 0.09 respectively and it was determined that

$$S_{max} = 0.2\, h_{sea}. \quad (5)$$

No universal value was found for h_{sea} so site-specific values were found by least squares fit to data sets for each site. x_{max} is the x location at which the exponential function is a maximum.

While S describes the amplitude of bars as a function of depth, the cosine term, $\cos[\theta(h_0) - \psi(t)]$, models the actual sand bar form. The bar phase structure can be found as

$$\theta(x) = \int_{x_{off}}^{x} \frac{2\pi}{L(x)}\,dx \quad (6)$$

where L(x) is the spatially-variable bar wavelength and the integral starts from the offshore limit of the domain and proceeds inward to every x, using the depth, h_0, at each x location. Bar wavelengths are surprisingly well predicted by an empirical relationship

$$L(h_0) = a_L \exp(b_L h_0(x)) \quad (7)$$

where best fit values of a_L and b_L are found to be 100 and 0.27, respectively.

The temporal phase, $\psi(t)$ is determined from the fact that bar crests (minimum depths) will occur when the argument of the cosine equals zero. Thus, if we can independently identify a bar position, x_b, we can find

$$\psi(t) = \theta(x_b) \quad (8)$$

where θ was found using Eq. (6). The final sum of the background and barred profile (Eq. (1)) is referred to as the "barred profile" and can be directly compared to measured bathymetries.

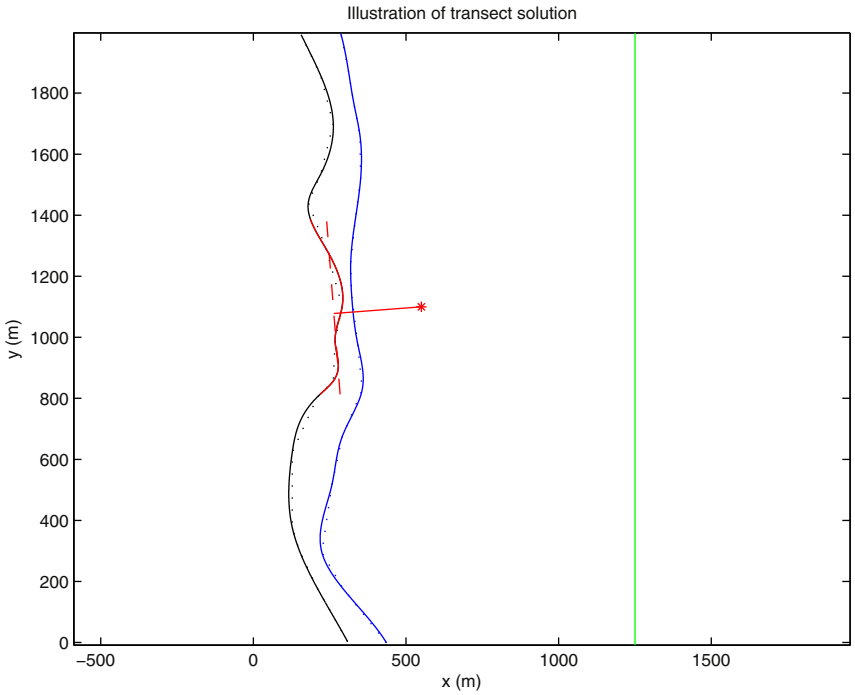

Fig. 1. Schematic of example test case. The shoreline is shown in black (dotted line shows original points while the solid line shows the spline-interpolated shoreline). The blue line indicates the digitized sand bar location and the green line shows an assumed deep contour (chosen to be 12 m deep for this synthetic case). The red asterisk marks the particular analysis point, x_p, y_p. The red dashed line is the best-fit shoreline within the alongshore region of interest while the solid red line is the cross-shore transect (which defines a line that extends offshore to the deep contour).

As was discussed in HLEV14, of the twelve parameters needed for implementation, seven were evaluated as constants in RWHKvE03. Four of the remaining five are determined by: the climatological beach slope at the shoreline, the depth and bottom slope at some location seaward of the active bar zone (likely obtainable from nautical charts), and the cross-shore location of the sand bar crest determined from, for example, the breaker location from optical images of the nearshore. The final parameter, h_{sea}, is site-dependent and must be estimated. In the absence of other information, Eq. (5) can be used based on an estimate of the maximum expected height of sand bars at any site of interest.

2.2. 2D implementation

Natural beaches can only rarely be considered longshore-uniform. Shoreline locations vary on a range of scales from cusps to large-scale shoreline curvature and sand bar position are typical longshore-variable with a variety of morphologies (e.g. Wright and Short, 1983). These longshore bathymetric variations change nearshore circulation in important ways (e.g. Wilson et al., 2010 among many others), yielding rips currents and cell circulation that are important to mixing and morphological evolution.

One concept for extending HLEV14 to two dimensions is to simply take profiles that are orthogonal everywhere to a longshore-variable shoreline orientation and averaging the offshore results with a spatial smoothing. However this method was discarded after it was found to be unstable and overly sensitive to details of shoreline orientation (depth estimates at any offshore location could be averages from a random mix of originating shoreline transect locations).

Instead, the following method was found to work. Instead of computing a suite of offshore transects for every shoreline position then averaging at every offshore position, it was assumed that each estimation point seaward of the shoreline "sees" the coast as roughly straight with an orientation that is the average over a longshore span whose length depends on the offshore distance. For large offshore distances, the coastal orientation should be thought of as the average over a large span whereas close to the beach the orientation is more localized. Given this mean coastal orientation, a normal transect can be determined between the estimation point and the corresponding averaged shoreline. From the intersection of this transect with a bar and offshore location a full barred bathymetry can be computed using HLEV14 from which the depth at the estimation point can be found. This is carried out one point at a time over a full 2D estimation grid (this may seem like a lot of wasted computation but bathymetries presented below took only an average of 120 s to compute on an average laptop).

Table 1
Dates and error statistics of the fourteen tested bathymetries computed from $\Delta h = h_{param} - h_{survey}$ (so positive Δh corresponds to parametric estimates being too deep). Bias and rms statistics are listed both for the entire region (shore to x = 700 m) and split into shallow (true depths < 3 m) and deep (true depths > 3 m). Median and 90% percentile of abs(Δh) are also shown.

Bathy date	Timex date	Bias (m)			rmse (m)			Median (m)	90% (m)
		All	<3 m	>3 m	All	<3 m	>3 m		
09/16/09	09/16/09	0.30	0.19	0.34	0.47	0.39	0.49	0.30	0.77
10/21/09	10/21/09	0.30	0.30	0.30	0.47	0.48	0.47	0.29	0.77
12/10/09	12/13/09	0.28	0.33	0.26	0.49	0.64	0.43	0.30	0.85
01/14/10	01/14/10	0.21	0.11	0.25	0.41	0.40	0.42	0.25	0.75
02/22/10	02/25/10	0.21	0.08	0.25	0.51	0.40	0.53	0.30	0.92
04/05/10	04/04/10	0.26	0.08	0.32	0.50	0.37	0.53	0.28	0.87
04/16/10	04/15/10	0.28	0.09	0.34	0.52	0.40	0.54	0.29	0.87
06/04/10	06/07/10	0.25	0.07	0.31	0.48	0.39	0.51	0.31	0.87
09/06/10	09/09/10	0.33	0.34	0.33	0.51	0.51	0.51	0.34	0.87
10/19/10	10/22/10	0.34	0.36	0.33	0.54	0.54	0.53	0.29	0.95
11/22/10	11/24/10	0.29	0.21	0.33	0.54	0.56	0.54	0.30	0.97
02/07/11	02/05/11	0.27	0.31	0.26	0.52	0.56	0.50	0.22	0.97
03/18/11	03/18/11	0.25	0.47	0.16	0.49	0.69	0.38	0.23	0.87
05/02/11	05/02/11	0.22	0.35	0.17	0.44	0.59	0.36	0.21	0.77
Mean		0.27	0.24	0.28	0.49	0.50	0.48	0.28	0.86

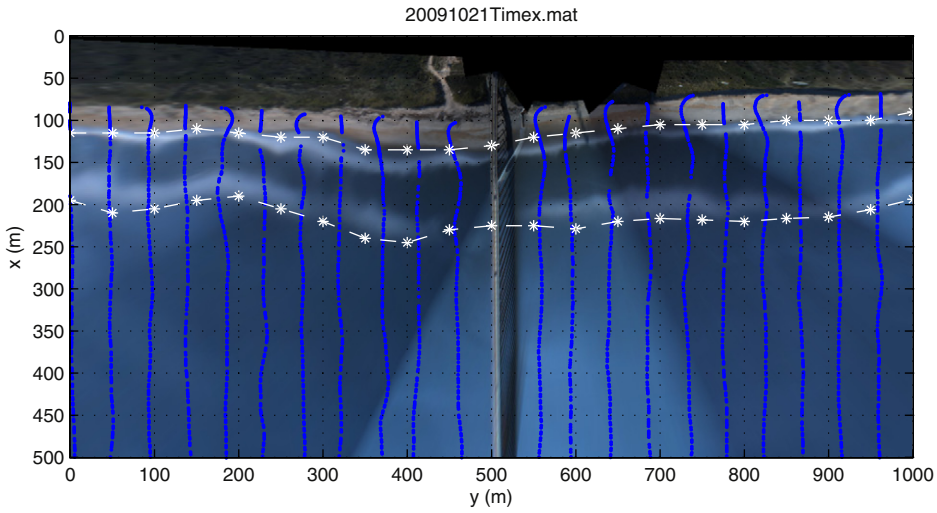

Fig. 2. Example rectified time exposure image for October 21, 2009. Blue points represent the tracks from the ground truth survey. The vertical feature at y = 515 m is the research pier. Shoreline locations extracted from survey data are shown by the white asterisks along the beach's edge while the estimated bar crest locations are the white asterisks overlying the white band of preferred breaking around x = 200 m.

The concept is illustrated in Fig. 1 where we are trying to estimate the depth at a particular offshore point, $[x_p,y_p]$, shown as a red asterisk in the figure. We assume the shoreline has been digitized from a rectified aerial photograph as a series of points, x_s, y_s and the foreshore beach slope has been estimated from local knowledge as $\beta_s(y)$. We wish to define a mean shoreline that would be "seen" by the offshore point as the best fit line (dashed near-vertical line in Fig. 1) to the shoreline data within $K * dx$ of y_p, where dx is the distance between x_p and the mean of the subset of shoreline x locations. For illustration we have used $K = 1$ (other choices are investigated later). Fig. 1 shows the selected subset of shoreline data as a red curved line (from $y_p - K * dx$ to $y_p + K * dx$) while the dashed red line shows the best linear fit to these points. This problem must be solved iteratively (guessing an offshore distance, then finding the shoreline subset, then improving the estimate of dx, until convergence).

Having identified a linear shoreline that is appropriate to a particular offshore location, the subsequent analysis is straightforward. A normal is found to the shoreline (solid straight red line in Fig. 1, having an orientation of $-1/m$, where m is the slope of the shoreline fit line, $x = my + b$). The intersection of the straight shoreline with this normal is found as x_0, y_0, and the along-transect distance, d, is found between this point and x_p, y_p. The along-transect distance, d_b, is found to the sand bar and the distance, d_d, is found to the deep contour. The offshore depth and slope at the deep location are found. From these values, a 1D barred profile can be found as in HLEV14 and the depth at along-transect distance, d, is interpolated. This process is carried out for every location in an analysis map grid that is seaward of the shoreline. Note that the intersection of the cross-shore transect with the bar or deep contours requires finding the two-line intersection for every line segment along the bar (or deep) contour and choosing the one that lies within the line segment (i.e. most will intersect outside of the domain of each point pair).

3. Field data tests

The above parametric barred beach form was compared against fourteen 2D beach surveys carried out at the FRF, Duck, North Carolina, under widely varying environmental conditions between September 2009 and May 2011 (dates listed in Table 1). Survey data were collected along 26 cross-shore transects with an alongshore spacing of 50 m and a

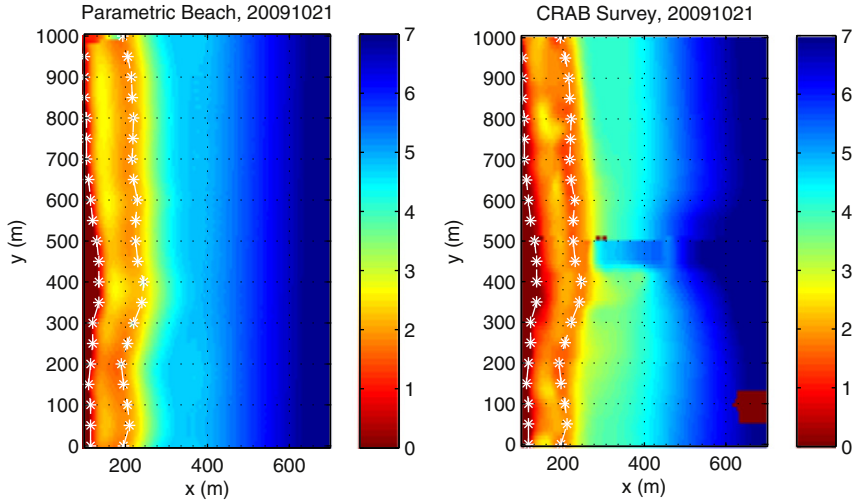

Fig. 3. Comparison of surveyed (right) and parametric (left) bathymetries. White lines show the shoreline and sand bar locations extracted from the survey data. The CRAB survey anomaly around y = 500 m is the poorly sampled trench below the pier and is ignored in statistical comparisons.

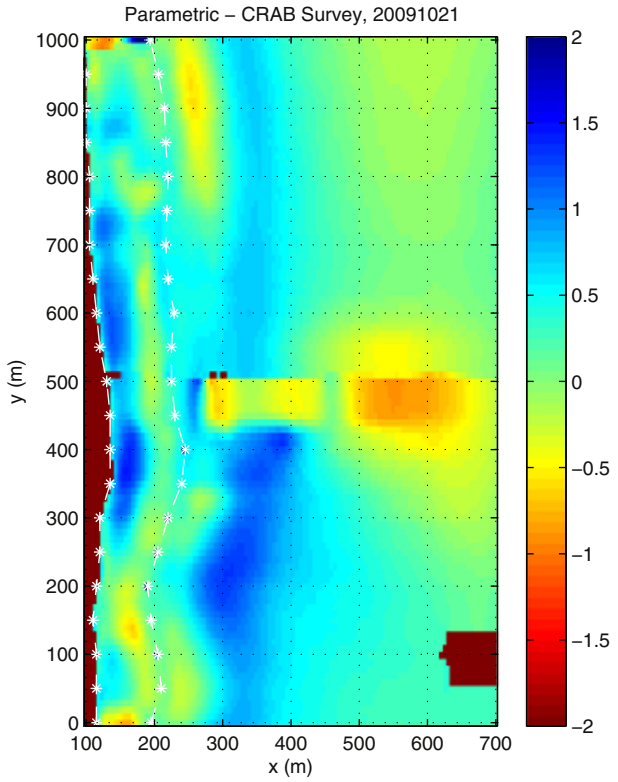

Fig. 4. Difference plot of parametric minus surveyed depths for October 21, 2009. The narrow band of error between x = 150 and 200 corresponds to a slight misplacement of the inner bar crest location. The blue-ish region around x = 350 is a slight over-estimated of depth in the offshore bar region. The region between y = 400 and 600 m should be ignored.

typical cross-shore sample spacing of 3.5 m. Transects extended from the dune base to 800 m offshore, with five transects extending to 2000 m. An example of the survey coverage is shown in Fig. 2. Birkemeier and Mason (1984) found that the vertical accuracy of FRF surveys is approximately 0.05 m. The local x coordinate extends in the cross-shore direction while y is oriented alongshore in a right hand coordinate system with z positive up. Survey data were interpolated onto a 5 by 10 m (cross and alongshore spacing) grid using loess interpolation with 25 and 50 m cross-shore and longshore smoothing.

The necessary inputs for the parametric model were found as follows. For initial testing, the shoreline and bar crest locations were found from measured bathymetries (initiation from time exposure images is discussed later in the paper). The shoreline was defined as the location for which depth equals mean sea level (z = 0). The bar crest location was determined as the first depth minimum seaward of the shoreline, with manual supervision to correct transects with monotonic depth increase. Longshore spacing was chosen to be 50 m, but is arbitrary (Fig. 2). Following the values chosen in HLEV14, the foreshore climatological beach slope, β_s, was taken as 0.10, the mean over all surveys (from HLEV14), while the value of h_{sea} was taken to be 4.5 m. The deep water variables were chosen from example survey data (but could easily have been taken from charts) as depth of 7.5 m at x = 700 and offshore bottom slope, β_0, of 0.0088. Offshore depths were assumed alongshore uniform. K was taken to be 1.0.

Fig. 3 shows an example comparison between a surveyed and a parametric bathymetry for October 21, 2009, a case of moderate longshore variability in shoreline and sand bar position. Anomalies in the surveyed bathymetry near y = 500 m, due to the known scour trench under the FRF pier, are poorly sampled in the survey and are not representative of natural beach processes. Performance statistics (below) therefore neglect the region between longshore distances 400 and 600, as is common practice.

The parametric bathymetry looks very similar to the survey, especially in shallow water. The overall structure of the shoreline and bar are well

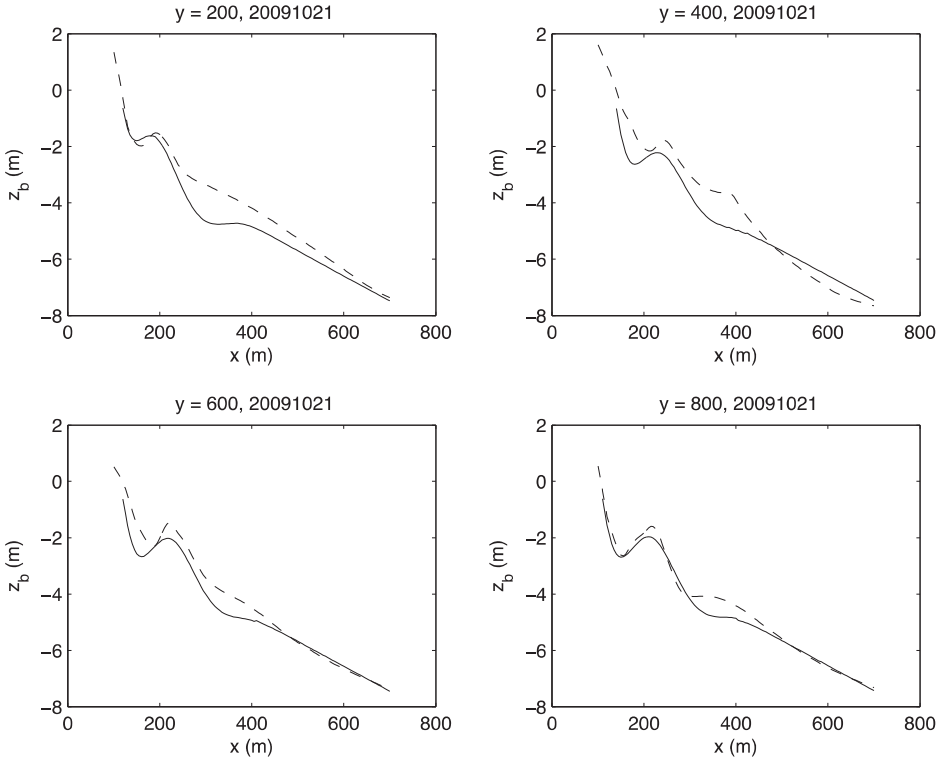

Fig. 5. Example profiles from Fig. 3 at y = 200, 400, 600 and 800 m. Solid (dashed) lines correspond to parametric (survey) estimates.

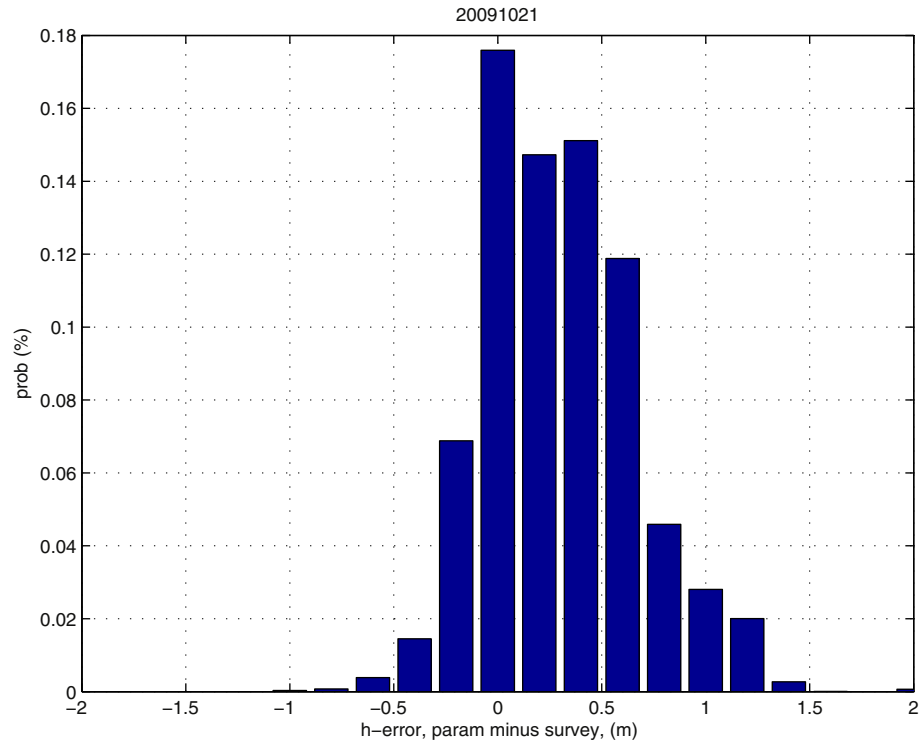

Fig. 6. Probability distribution of depth errors (predicted – survey) for the 10/21/09 survey. Positive values correspond to over-prediction of depth.

represented and longshore variations in the trough are reasonable. A low-amplitude offshore bar is present but is slightly deeper than in the survey. Fig. 4 shows a difference plot of parametric minus survey depths (positive values correspond to over-estimates of depth in the parametric bathymetry) while Fig. 5 shows transects of parametric and surveyed estimates at four longshore locations. Overall, the parametric form does a very good job of representing the 2D survey bathymetry. The most visually apparent error (aside from the deep trench below the pier) is due to a slight misplacement of the cross-shore bar position (between x = 150 and 200 m). To seaward (x ~ 350 m) the parametric form over-predicts depth by roughly 1 m to the south but is surprisingly accurate to the north (y = 600, 800 m).

Fig. 6 shows a histogram of the prediction error. The slight bias toward over-prediction of depth is apparent, but there are no particularly large anomalies. The bias and rms error over the full domain are 0.30 and 0.47 m, respectively. The median value of the absolute error was 0.29 m while the 90% percentile of absolute error was 0.77 m (i.e. 90% of errors were less than this value). The error statistics were also partitioned by depth to determine if performance was better in shallow (h < 3 m) or deeper (h > 3 m) regions. Both bias and rmse were essentially depth independent for this case.

Statistics for each of the fourteen surveys are shown in Table 1. The results are quite consistent from survey to survey. On average, the bias is a 0.27 m over-prediction with an rms error of 0.49 m. The average median and 90th percentile absolute errors are 0.28 and 0.86 m, respectively. The bias is slightly lower in shallow water (<3 m; 0.24 versus 0.28 m) while the rms error is essentially the same in both regions (0.50 versus 0.48).

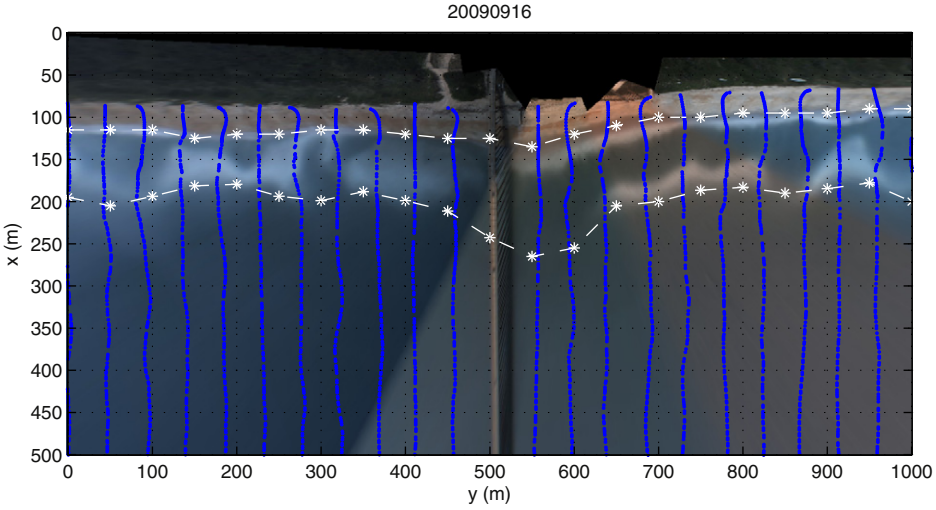

Fig. 7. Rectified time exposure for 09/16/09, one of the most complex bar configurations in the study.

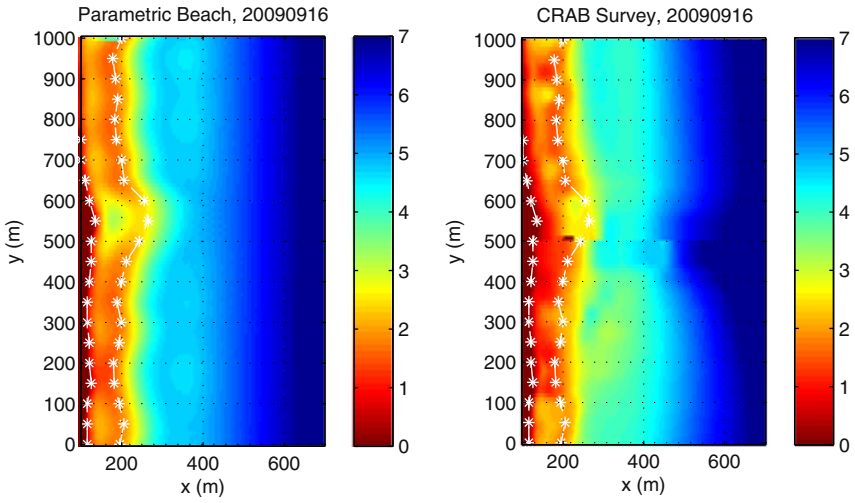

Fig. 8. Parametric (left) and surveyed (right) bathymetries for 09/16/09. Despite the obvious three-dimensionality of the bar system and shoreline (Fig. 7), the predicted bathymetry is quite good, with error statistics there are typical of all cases (Table 1).

Fig. 7 shows the most complex bar system in the data set (09/16/09) while Fig. 8 shows the corresponding comparison of parametric and surveyed bathymetries. The 2D parametric bathymetry is a very good approximation of the survey, with error statistics that are roughly the same as the global averages (Table 1).

Fig. 9 shows one further case from 04/16/10, another case where the survey bathymetry shows strong longshore variability. The parametric bathymetry represents well the alongshore variability but cannot represent rip channels that have been cut through the bar at y = 190 and 750 m.

The best value of K is unknown. A value smaller than the default value of 1.0 would make the parametric bathymetry more sensitive to shoreline details while a large value reduces this sensitivity. Performance statistics were computed for values of K of 0.5 and 2.0, so spanning a factor of four. The statistics of the fit were found to be quite insensitive (Table 2).

It should be realized that for a generally straight beach such as Duck, shoreline curvature could be reasonably ignored - after all, the results of HLEV14 were all based on 1DH cross-shore transects with no sensitivity to shoreline curvature. However, there are negative consequences of adapting the 1DH approach for longshore variable beaches. First, every detail of shoreline variability will be carried throughout the profile, so the position of the crest of an offshore sand bar will vary just as much as the shoreline, an unrealistic behavior (although subtle in terms of error since offshore features are usually low sloping). Second, for cases with more significant shoreline curvature like a pocket beach, the sensible variability of shore normal direction is required for realistic bathymetry and hydrodynamics.

For real applications, the surveyed bathymetry will be unknown (why would you then approximate it?). Thus, shoreline and sand bar input data must be found in other ways, most likely from remote sensing data. This was tested by using rectified time exposure images collected by the Duck Argus Station (for example, Figs. 2 and 7) and manually digitizing the shoreline and sand bar locations by clicking on the image. This has previously been shown to provide a good approximation, although some cross-shore misplacement can occur depending on the wave conditions (e.g. Lippmann and Holman, 1989; Plant and Holman, 1997; van Enckevort and Ruessink, 2001). This was done for each of the fourteen survey times. For several cases, waves were too small to break over the sand bar on the survey date so the closest time exposure with usable signals was chosen, sometimes up to three days different from the ground truth survey date (time exposure dates are listed in Table 1). Parametric bathymetries were computed for each case and the statistics found (last line, Table 2). Surprisingly, bulk statistical performance was

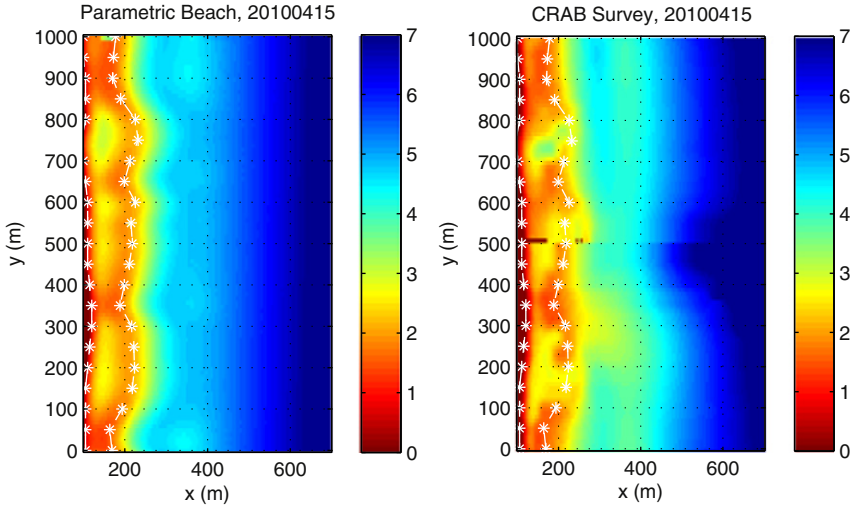

Fig. 9. Predicted (left) and surveyed (right) bathymetries from 04/16/10.

Table 2
Average performance statistics for different values of K (first three rows). The final row shows the performance statistics when the input shoreline and bar locations were manually picked from rectified time exposure images instead of the surveyed bathymetry.

K	Bias (m)			rmse (m)			Median (m)	90% (m)
	All	<3 m	>3 m	All	<3 m	>3 m		
0.5	0.27	0.23	0.28	0.49	0.49	0.48	0.28	0.86
1.0	0.27	0.24	0.28	0.49	0.50	0.48	0.28	0.86
2.0	0.27	0.24	0.28	0.49	0.50	0.48	0.28	0.86
Timex, K = 1	0.25	0.10	0.29	0.49	0.48	0.49	0.29	0.86

no worse using these approximate inputs than using those derived from surveyed bathymetries.

4. Discussion

The 2D parametric algorithm does a very good job producing realistic bathymetries based only on simple inputs of shoreline and sand bar locations, a shoreline climatological slope and some offshore depth and slope at a location that is seaward of the active sand bar region (anywhere seaward of 8 m depth is usually adequate). These predictions are a great improvement over traditional power law or exponential beach forms due to the inclusion of sand bars that will strongly influence nearshore wave breaking and the resulting circulation. The parametric form can well represent the longshore variability that is important for causing rips currents and cell circulation although rip channels that are cut through a sand bar cannot be modeled.

The algorithm can be used in two general ways. The first is for general or even conceptual studies where the user simply needs a realistic bathymetry to study processes. This is the traditional role of equilibrium beach profiles – for instance, the $x^{2/3}$ profile is often used for this type of study since it represents the typical concave average bathymetry of ocean beaches. However the lack of the sand bars makes hydrodynamic predictions on these simpler profiles unrealistic. Since no sand bar location is known, different bar placements can be explored at will. The second application is to represent a specific beach for which measured bathymetry is poor or completely lacking. This is often the case for Navy applications where bathymetry is needed for operational planning but is unavailable. This algorithm could provide a realistic substitute based only a few inputs that could reasonably be estimated or guessed. Of course, the estimated bathymetries would not be as good as measurements, but they are surprisingly good.

The largest numerical errors are often due to a cross-shore misplacement of the sand bar position (for instance the slight misplacement of the bar location in Fig. 3 and resulting alongshore anomaly between x = 150 and 200 m in Fig. 4). The associated increase in the error statistics due to a realistic bar form shifted slightly in the cross-shore is misleading since both the bathymetric form and any resulting hydrodynamics will still be realistic but slightly shifted in the cross-shore.

Digitization of shoreline and sand bar locations from optical imagery is necessarily subjective. For a steep beach like Duck, the shoreline can usually be fairly accurately found. However, at other times and locations a small low tide terrace can be present and shorelines must be estimated to the landward of the terrace break (e.g. around y = 600, Fig. 7). Both the shoreline and sand bar location digitization should be based on mean tide time exposure images since both signals will vary with the tide. However, preference in this case was given instead to finding time exposure images that best showed usable breaking patterns over the offshore sand bar location (usually a low tide).

Most practical applications of this algorithm will be based on snapshots of wave breaking rather than time exposure images. Fig. 10 shows a rectified snapshot from 10/21/09, the initial case discussed above. White dashed lines correspond to the shoreline and sand bar locations digitized from the surveyed bathymetry in Fig. 3. In this case there is sufficient signal in the single snapshot to allow reasonable estimates of shoreline and sand bar locations. In general the use of snapshots rather than time exposures should degrade the final product somewhat. However a user should be able to judge the merit of their choices. In all cases, the most likely resulting error will be a cross-shore misplacement of sand bars and the resulting bathymetries and hydrodynamics will still be more realistic than for unbarred bathymetries.

The current version of the analysis assumes that the longshore direction corresponds roughly to the y-axis, i.e. the shoreline, bar and deep input data can be reasonably expressed as a function of y. Under more complex situations, other choices may need to be made, for example to frame the problem as a function of a series of longshore line segments. Similarly, the alongshore spacing of input data is arbitrary. It must be dense enough to represent important shoreline variability and, while densely spaced inputs are fine, they may needlessly increase computation time. The computation time for these cases averaged 120 s using a low level desktop computer.

The algorithm depends on and may be sensitive to a number of parameters. The most sensitive is h_{sea}, the seaward limit of significant sand bar activity. HLEV14 investigated this dependence and found that increasing h_{sea} lead to a larger amplitude sand bars that continued

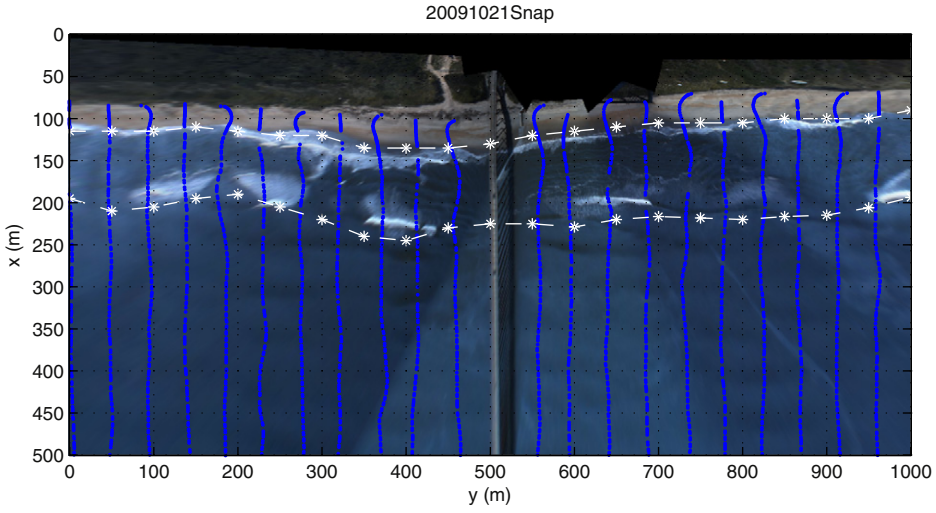

Fig. 10. Merged rectified snapshot that corresponds to the same time as the time exposure in Fig. 3. White dashed lines again correspond to the shoreline and bar location digitized from the surveyed bathymetry. Wave breaking over the sand bar is more sporadic in the snapshot but would still yield quantifiable shore and bar locations.

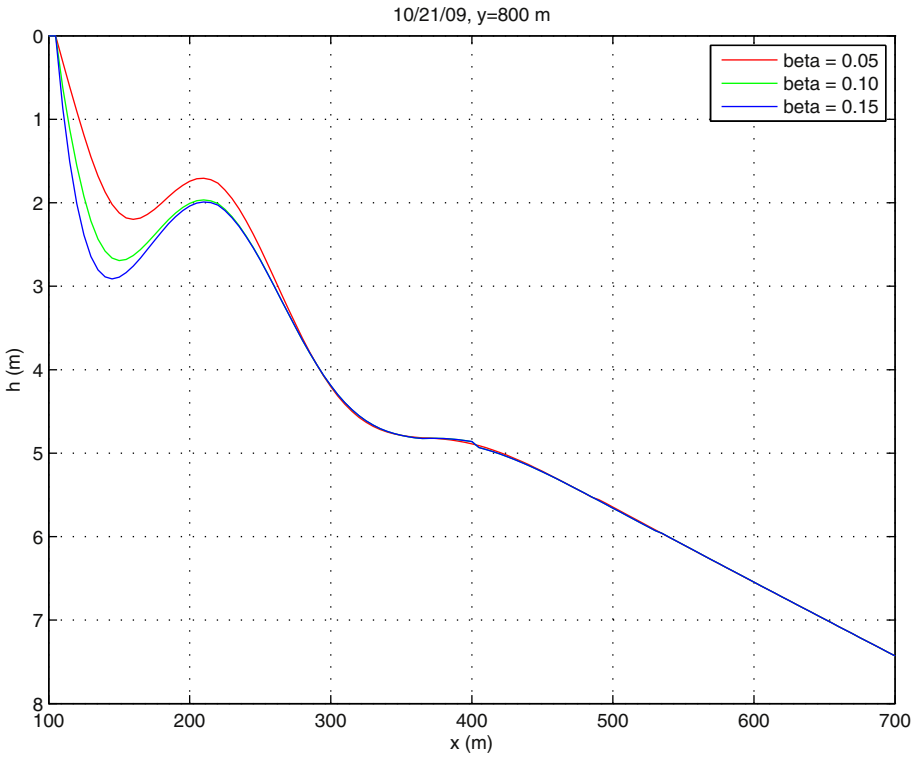

Fig. 11. Example profiles showing the sensitivity of predicted bathymetries on choices of shoreline beach slope, β_s.

further seaward. This would lead to errors offshore but would have little impact closer to the beach where the surf zone is most active and interesting. In the absence of any information on the best choice for h_{sea}, it is possible to estimate the maximum expected amplitude of sand bars and use Eq. (5) to find h_{sea}.

Errors in the shoreline location have obvious consequences of spatially offsetting the resulting bathymetry. Similarly, errors in the depth at some offshore location simply deepen or shallow the profile slightly with small resulting effects in bar positioning away from the input sand bar location. However, the input bar position will usually be one that is detected in shallow water, the location where conditions are usually of the greatest interest, so this is a fairly innocuous error. The remaining unknown sensitivities are due to errors in the shoreline and offshore slopes.

The role of the shoreline beach slope, β_s, is shown in Fig. 11. The primary effect of changing β_s is to change the depth in the trough region, close to the beach. The location of the bar is unchanged (since it is an input), although the bar crest depth is slightly affected.

The role of the deep-water slope, shown in Fig. 12, is larger. The active bar zone and the amplitudes of sand bars are dependent on the depth of the background profile, h_0, and are limited to a depth span from 0 to h_{sea}. Choosing a too shallow offshore slope will make the cross-shore width of this region very narrow so that bar perturbations will appear to be small (see $\beta = 0.006$ case in Fig. 12). In this sense, the choice of this slope has an indirect impact on the bar amplitudes. It is also quite possible to choose an offshore slope that is too steep, so would intersect the beach above sea level (i.e. the beach would need to be convex up to meet the shoreline, a possible but unlikely scenario). In this case the algorithm defaults to a background profile that is a plane beach between the deep point and the shoreline. Realistic bars are still predicted.

The deep-water input can be located anywhere seaward of the active bar zone, even kilometers away. It simply acts as a boundary condition for solving for the background profile, h_0. Choosing a distant location does not increase computation time, although the greater the offshore distance, the less likely it is that shore normal transects will intersect a spatially-limited deep water contour (this problem can be resolved by inputting a very long offshore contour). Various options exist for finding deep-water depths and slopes including digital nautical charts, alternate remote sensing methods such as multi-spectral methods, or even rough estimates from experienced geologists.

5. Conclusions

This paper describes and tests a method for approximating realistic 2DH nearshore bathymetry in the absence of bathymetric measurements. It is an improvement over simple monotonic equilibrium bathymetries due to the addition of realistic sand bars and the associated great improvements in hydrodynamic predictions. It extends the 1DH model of Holman et al. (2014) in allowing for alongshore variability. Model inputs include the position and climatological beach slope of the shoreline, the location of a sand bar crest and the location and bathymetric slope at any offshore location that is seaward of the zone of active sand bars.

The model was tested against 14 area surveys collected at Duck, NC, over a two-year period, each spanning 500 m in the cross-shore and 1000 m in the longshore. Input data for initial tests were extracted from survey data and a single historical deep-water survey with a later tests based on inputs extracted from remote sensing data. The mean bias over the entire region and data set was 0.27 m with an rms error of 0.49 m. Roughly 90% of the estimates were within 0.86 of the ground truth. The largest source of error was occasional cross-shore misplacements of otherwise realistic looking sand bars. Hydrodynamic predictions using these bathymetries would be a substantial improvement over those from monotonic or even barred 1DH equilibrium proxy bathymetries.

Acknowledgements

The work was supported by the Office of Naval Research through base funding of the Naval Research Laboratory.

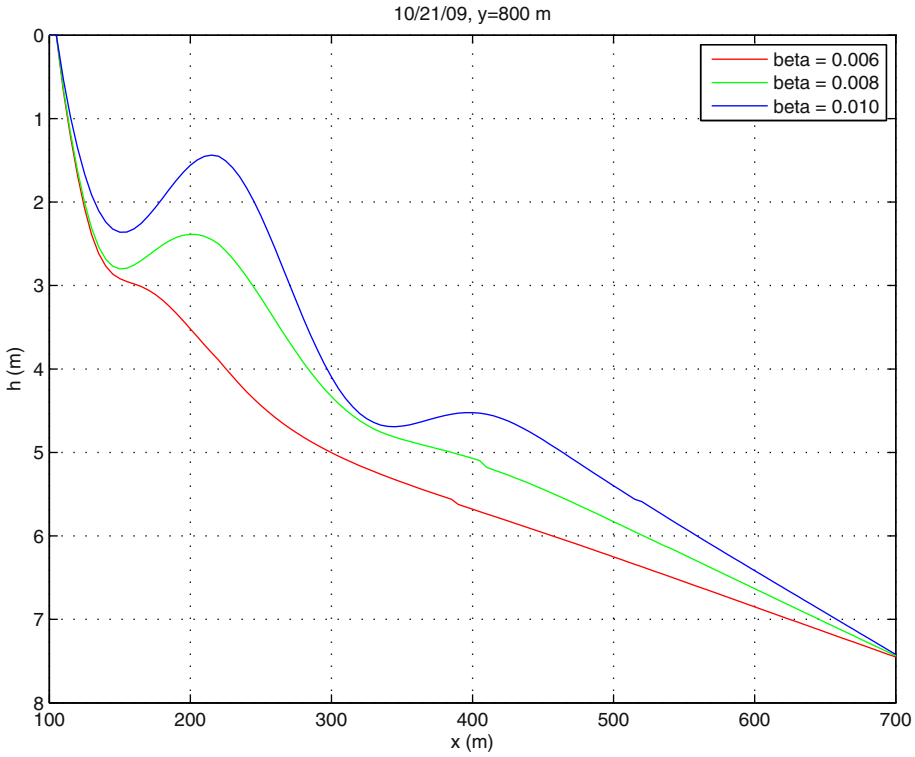

Fig. 12. Sensitivity of bathymetry to the chosen deep-water beach slope. For comparison, the value used for the Duck tests was 0.0088. The inner bar crest position appears to change, despite being a fixed input. In fact, the location of the maximum bar perturbation does remain fixed, but not the location of the minimum depth.

References

Birkemeier, W.A., Mason, C., 1984. The CRAB: a unique nearshore surveying vehicle. J. Surv. Eng. 110, 1–7.

Bodge, K.R., 1992. Representing equilibrium beach profiles with an exponential expression. J. Coast. Res. 8 (1), 47–55.

Bruun, P., 1954. Coast erosion and the development of beach profiles. Technical Memorandum (Rep).

Dean, R.G., 1991. Equilibrium beach profiles: characteristics and applications. J. Coast. Res. 7, 53–84.

Holman, R.A., Lalejini, D.M., Edwards, K., Veeramony, J., 2014. A parametric model for barred equilibrium beach profiles. Coast. Eng. 90, 85–94.

Inman, D.L., Elwany, H.S., Jenkins, S.A., 1993. Shorerise and bar-berm profiles on ocean beaches. J. Geophys. Res. 98 (C10), 18181–18199. http://dx.doi.org/10.1029/93JC00996.

Komar, P.D., McDougal, W.G., 1994. The analysis of beach profiles and nearshore processes using the exponential beach profile form. J. Coast. Res. 10 (59-69).

Larson, M., Kraus, N.C., 1989. SBEACH: numerical model to simulate storm-induced beach change (Rep).

Lippmann, T.C., Holman, R.A., 1989. Quantification of sand bar morphology: a video technique based on wave dissipation. J. Geophys. Res. 94 (C1), 995–1011.

Ozkan-Haller, H.T., Brundidge, S., 2007. Equilibium beach prfile concept for Delaware beaches. J. Waterw. Port Coast. Ocean Eng. 133 (2), 147–160. http://dx.doi.org/10.1061/(ASCE)0733-950X.

Plant, N.G., Holman, R.A., 1997. Intertidal beach profile estimation using video images. Mar. Geol. 140, 1–24.

Ruessink, B.G., Wijnberg, K.M., Holman, R.A., Kuriyama, Y., van Enckevort, I.M.J., 2003. Inter-site comparisons of interannual nearshore bar behavior. J. Geophys. Res. 108. http://dx.doi.org/10.1029/2002JC001505.

van Enckevort, I.M.J., Ruessink, B.G., 2001. Effect of hydrodynamics and bathymetry of video estimates of nearshore sand bar position. J. Geophys. Res. 106 (C8), 16969–16979.

Wilson, G.W., Özkan-Haller, H.T., Holman, R.A., 2010. Data assimilation and bathymetric inversion in a two-dimensional horizontal surf zone model. J. Geophys. Res. 115 (C12). http://dx.doi.org/10.1029/2010JC006286.

Wright, L.D., Short, A.D., 1983. Morphodynamics of beaches and surf zones in Australia. In: Komar, P.D. (Ed.), CRC Handbook of Coastal Processes and Erosion. CRC Press, Boca Raton, pp. 35–64.